The ultrasonic method of hardboard testing

S. V. Augutis, A. Dumčius, D. Gailius, D. Styra, S. Jačėnas

Department of electronics and measurement systems
Kaunas University of Technology

Introduction

When manufacturing wood fiberboard panels (hardboard panels) one should retain in the permissible limits all their shown parameters. To secure these parameters and effective control of the production process information about their basic parameters already in the very production line is necessary. Therefore, effective methods of these hardboard parameters determination, based upon non-destructive testing are necessary. In this paper the non-destructive measurement method for determination of hardboard bending strength (Modulus of Rupture) is offered.

Standard determination method of bending strength

One of the most important hardboard (HB) technical parameters is their bending strength (in MPa), which is determined by breaking in two (500x50 mm dimension) specimen by a special arrangement. In many countries, where hardboard is manufactured, this method has been legalized by national standards.

The bending strength is being determined by bending a specimen placed on supports until it breaks and is fixed the maximum bending (breaking in two) force P_{max}. A measurement diagram is shown in Fig. 1.

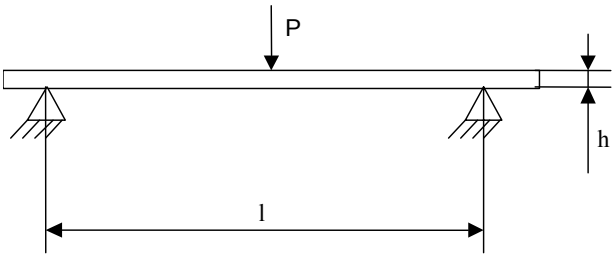

Fig. 1. **Standard bending strength measurement diagram**

The strength is assessed by bending tensions corresponding maximum force P_{max} the breaking specimen in two parts:

$$\sigma_b = \frac{1{,}5P_{\max}}{b}\frac{l}{h^2}, \qquad (1)$$

where l is the distance between the supports, h is the thickness of the sample, b is the width of the sample, P_{max} is the force of breaking in two parts.

In order to determine the bending strength by this method one should cut out from various HB places four specimens, each of them from different HB quarter: two specimens are being cut out along the HB, i.e. in the machine direction, the other two- in the cross-direction. One from each specimen couples is broken from one side (face), the other- from another side. The HB bending strength is determined, having calculated the average strength value out of four specimens.

The relative extended bending tensions uncertainty may be expressed on the basis of (Eq.1) as

$$U_\sigma = 2\cdot\sqrt{\left(\frac{\Delta P}{P}\right)^2+\left(\frac{\Delta l}{l}\right)^2+\left(\frac{\Delta b}{b}\right)^2+\frac{1}{3}\left(2\frac{\Delta h}{h}\right)^2}, \qquad (2)$$

where $\frac{\Delta P}{P}$, $\frac{\Delta l}{l}$ and $\frac{\Delta b}{b}$ are the relative standard measurement uncertainties corresponding to the force, distance between supports and specimen width; Δh is the quantization error of the specimen thickness measurement; the error distribution is regarded to be even.

In reality, during the measurement of the strength we attain

$$\frac{\Delta P}{P}=10^{-2}\ ;\quad \frac{\Delta l}{l}=2\cdot10^{-3}\ ;\quad \frac{\Delta b}{b}=10^{-2};\ \Delta h = 0{,}1\text{ mm}.$$

Then, when h=3mm, we obtain

$$U_\sigma = 7{,}5\cdot10^{-2}\ .$$

If σ_b = 40 MPa (typical value), then at the probability 0,95 the true σ_b value will be

$$37\text{ MPa} < \sigma_b < 43\text{ MPa}.$$

Ultrasonic symmetric Lamb waves method

The essence of this method is that the velocity propagation of ultrasonic waves depends upon their propagation environment Young modulus, density and Poisson's ratio. The symmetric Lamb waves have a very good feature - their velocity does not depend upon thickness of the sheet when thickness is less than wavelength. Then the velocity may be expressed as

$$v = k\sqrt{\frac{E}{\rho}} \qquad (3)$$

where v is the velocity of ultrasonic waves propagation, E is the material elasticity modulus, ρ is the material density, k is the proportionality coefficient.

Taking into account this fact and also initial investigation results during which Lamb waves excitation, attenuation and their frequency features were examined, there has been chosen the frequency about 50 kHz and the measurement base 400 mm. The measurement diagram is shown in Fig. 2.

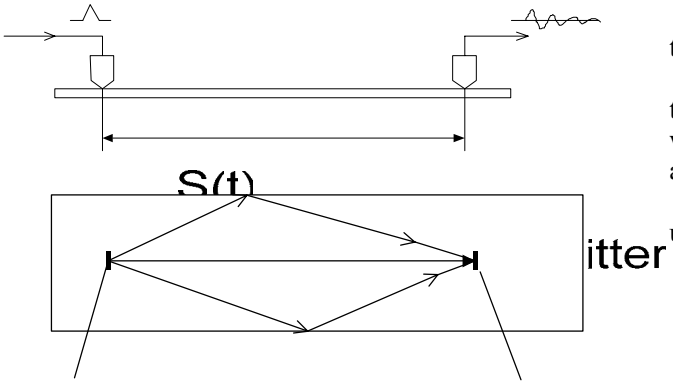

Fig. 2. **Measurement diagram and Lamb waves propagation paths**

The wave propagation time T_x is measured as shown in Fig. 3, from the transmitter impulse start till the receiver signal passing through the zero level.

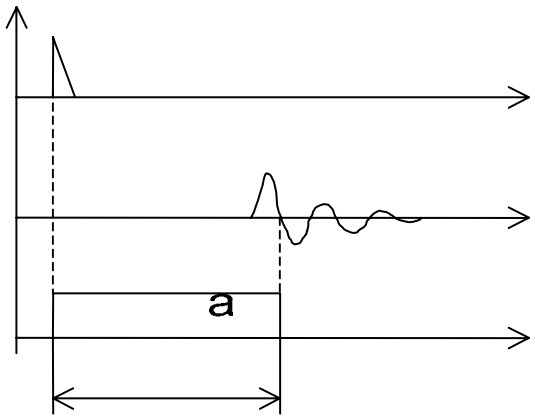

Fig. 3. **Measurement of wave propagation time**

The measurement channel will influence the propagation time measurement accuracy. To investigate this influence we have proposed the measurement channel model.

Model of the measurement channel

The measurement channel consists of the pulse generator, the piezoelectric Lamb waves transmitter, the segment of the plate under a test and the piezoelectric Lamb waves receiver. The structure of the channel is shown in Fig. 4.

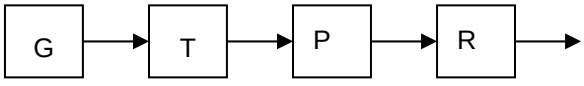

Fig. 4**. Measurement channel structure: G-generator, T- transmitter, P – plate, R- receiver**

The two conditions determine that low frequency Lamb waves must be used:

1. Attenuation in the plate increases when frequency increases;
2. The wavelength of the symmetric Lamb waves must be longer than the thickness of the plate. The influence of the plate thickness is avoided in this case.

Considering these conditions, the center frequency of the measurement channel must be about 40 kHz.

We will use resonant bimorph type piezoelectric transducers both for excitation and reception of Lamb waves. The electric capacitance of these transducers is about 2 nF, and mechanical quality factor 5 to 15.

For electrical excitation of the transmitter we have used the circuit showed in the Fig. 5.

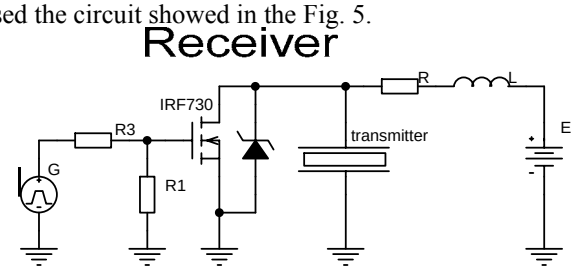

Fig 5. **Transmitters exciting circuit**

The MOSFET transistor is opened by variable duration pulses. The exciting voltage waveform on the transmitter was calculated by Pspice software, when L=2,7 mH , R=22Ω and τ_i=100μs, MOSFET type IRF730 and is shown in Fig. 6

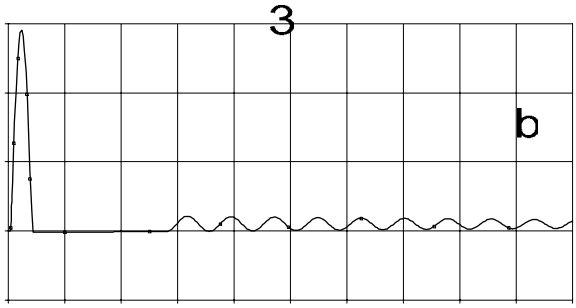

Fig. 6**. The exciting electric signal waveform**

This waveform differs little from the half sine pulse, corresponding to an ideal case.

Free vibrations may be damped using additional diode circuits, or by choosing proper L and R values, or by choosing duration of the exciting pulse. In Fig. 7 is shown how the ratio of main and following pulses amplitudes depends on duration of the exciting pulse. From these results we can see, that the preferable duration of the exciting pulse is τ_i=(70-100) μs, when L=2,7 mH and R=22 Ω.

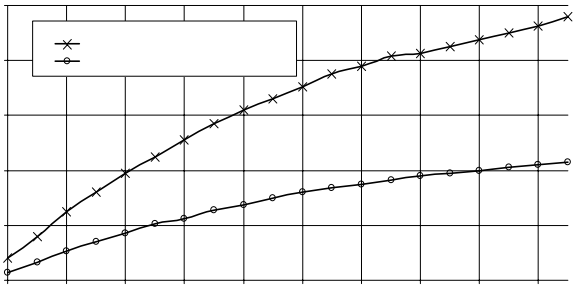

Fig. 7. **The dependence of the ratio of the main pulse amplitude to the other pulses amplitudes (baffling pulses) versus duration of the gate opening pulse τ_i.**

The electric model of the electromechanical part of the transmitter is shown in Fig. 8.

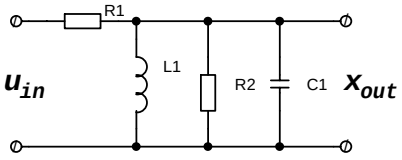

Fig. 8. **Electrical model of transmitter**

The transfer function of the transmitter is:

$$K_T(p) = \frac{1}{C_1 \cdot R_1} \cdot \frac{p}{(p - p_1) \cdot (p - p_2)}, \quad (4)$$

where

$$p_1 = \frac{-L_1R_1 - L_1R_2}{2L_1C_1R_1R_2^2} + \frac{\sqrt{L_1^2R_1^2 + 2L_1^2R_1R_2 + L_1^2R_2^2 - 4L_1C_1R_1^2R_2^2}}{2L_1C_1R_1R_2^2} \quad (5)$$

$$p_2 = \frac{-L_1R_1 - L_1R_2}{2L_1C_1R_1R_2^2} - \frac{\sqrt{L_1^2R_1^2 + 2L_1^2R_1R_2 + L_1^2R_2^2 - 4L_1C_1R_1^2R_2^2}}{2L_1C_1R_1R_2^2} \quad (6)$$

The quality of the resonant circuit depends on the force applied to the transmitter.

The transfer function of the plate:

$$K_p = \frac{k_0}{1 + p \cdot T} \cdot e^{p\tau}; \quad (7)$$

where T reflects damping dependence upon the frequency, and τ is the wave delay in the plate.

The electric model of the electromechanical part of the receiver is shown in Fig. 9.

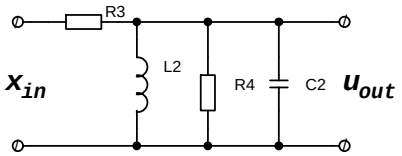

Fig. 9**. Electrical model of receiver**

The transfer function of the receiver is:

$$K_3(p) = \frac{1}{C_2R_3} \cdot \frac{p}{(p - p_3) \cdot (p - p_4)}; \quad (8)$$

where

$$p_3 = \frac{-L_2R_3 - L_2R_4}{2L_2C_2R_3R_4^2} + \frac{\sqrt{L_2^2R_3^2 + 2L_2^2R_3R_4 + L_2^2R_4^2 - 4L_2C_2R_3^2R_4^2}}{2L_2C_2R_3R_4^2}$$

$$p_4 = \frac{-L_2R_3 - L_2R_4}{2L_2C_2R_3R_4^2} - \frac{\sqrt{L_2^2R_3^2 + 2L_2^2R_3R_4 + L_2^2R_4^2 - 4L_2C_2R_3^2R_4^2}}{2L_2C_2R_3R_4^2} \quad (9)$$

Thus, the measurement channel part from the transmitter input to the receiver output is described by the transfer function:

$$K(p) = K_T(p)K_p(p)K_R(p) = \frac{k_0}{C_1R_1C_2R_3} \frac{p^2e^{-p\tau}}{(p - p_1)(p - p_2)(p - p_3)(p - p_4)(1 + pT)} \quad (10)$$

The pulse response is:

$$h(t) = \frac{k_0}{C_1R_1C_2R_3} \cdot \left[\begin{array}{c} \frac{p_1^2e^{p_1(t-\tau)}}{(p_1 - p_4)(p_1 - p_3)(p_1T + 1)(p_1 - p_2)} \\ \frac{-p_2^2e^{p2(t-\tau)}}{(p_1 - p_2)(p_2 - p_4)(p_2 - p_3)(p_2T - 1)} \\ \frac{Te^{\frac{-(t-\tau)}{T}}}{(p_1T + 1)(p_2T + 1)(p_3T + 1)(p_4T + 1)} \\ \frac{p_3^2e^{p3_1(t-\tau)}}{(p_1 - p_3)(p_2 - p_3)(p_3 - p_4)(p_3T + 1)} \\ \frac{-p_4^2e^{p_4(t-\tau)}}{(p_1 - p_4)(p_3 - p_4)(p_2 - p_4)(1 + p_4T)} \end{array} \right] \quad (11)$$

When the half sine form pulse is fed to the transmitter, the waveform on the receiver output we can calculate from the convolution of the system pulse response and the input signal [3].

$$S_{out}(t) = \int_0^t S_{in}(\tau) \cdot h(t - \tau)d \quad (12)$$

The examples of calculations are shown bellow.

The delay time in the measurement channel is τ and the measured time till the output signal zero level crossing instant is τ_1. The difference

$$\Delta\tau_1 = \tau_1 - \tau \quad (13)$$

we shall call the propagation time.

The calculated dependencies of this propagation time on the qualities of the transmitter and receiver resonant circuits are shown in Fig. 10., on the receiver resonant circuit quality in Fig. 11, on the plate damping time constant T in Fig. 12, and on the receiver resonant circuit resonant frequency- in Fig. 13, all other parameters were constant.

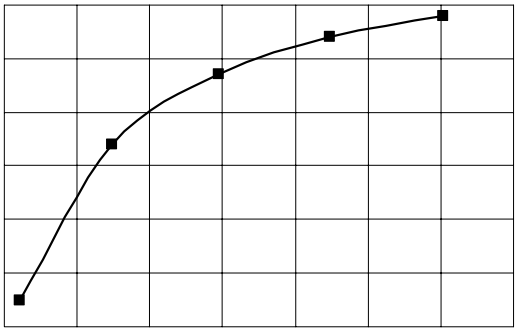

Fig 10. **Propagation time dependence on the resonant circuits quality**

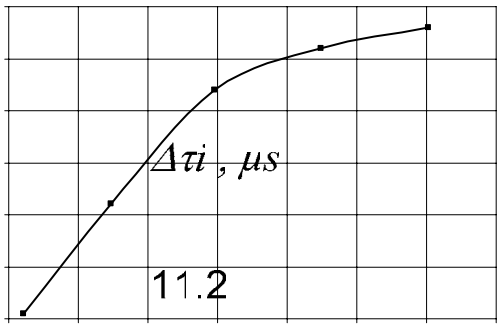

Fig. 11. **Propagation time dependence on the receiver resonant circuit quality**

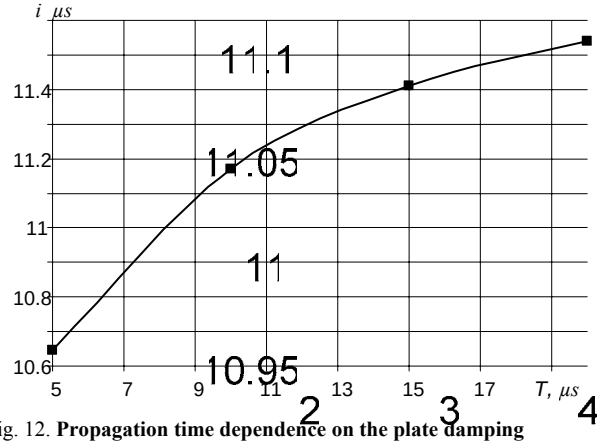

Fig. 12. **Propagation time dependence on the plate damping**

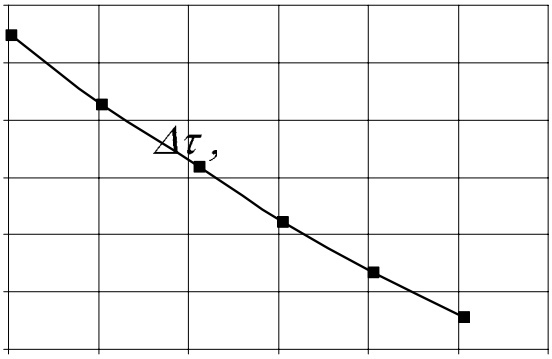

Fig. 13**. Propagation time dependence on the receiver resonant circuit frequency**

The calculated dependencies show stabilization of the measured propagation time when the resonant circuits quality is big enough. The recommended resonant circuits quality is $Q_{1,2} \geq 4$.

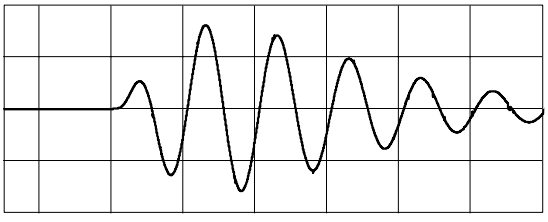

Fig. 14. **The signal on the receiver output circuit, when $L_1=L_2=$ 10 mH, $C_1=C_2=$ 1 nF, $R_2=R_4=$ 15 kΩ**

The resonant frequencies of the resonant circuits have considerable influence on the propagation time shift (Fig. 14). The transmitter and receiver resonant frequencies will depend on the interaction between them and the plate, namely from the pressing force. Consequently, both the transmitter and the receiver must be manufactured so, that the pressing forces will be constant.

For verification of the modeling results the experimental measurement were carried out. The results of these measurements are shown in Fig. 15 and 16.

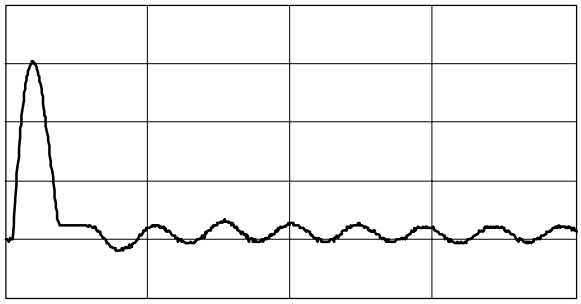

Fig. 15. **Experimental exciting electrical signal**

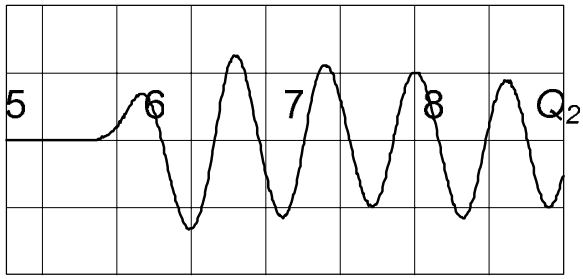

Fig. 16. **Experimental receiver output signal**

The measured signal at the receiver output shows that real quality of the transmitter and receiver circuits is more than 5.

On the basis of the modeling and experimental results we may evaluate uncertainty of the propagation time measurement.

The measurement uncertainty U_{Tx} consists of the following basic components: component U_{T0} that causes passing through zero instant determination in a comparator, digital measurement technique stipulated quantization component U_{Tk} and a component of measurement basis change U_{Tl} (instrument positioning, surface influence, etc.). The distribution of the component U_{Tk} is kept to be even, while others components distributions – normal.

Thus, the extended uncertainty of the propagation time measurement is

$$U_{Tx} = 2 \cdot \sqrt{U_{T0}^2 + \frac{1}{3} U_{Tk}^2 + U_{Tl}^2} \,. \qquad (14)$$

Considering that the standard uncertainty of the base l is $U_l = 0{,}22$ mm, the velocity in the plate is 2200 m/s, we obtain $U_{Tl} = 10^{-7}$ s. We easily obtain U_{Tk} 10^{-8} s.

By measuring the propagation time close to the HB edge or in band like HB specimen, due to reflections the received signal may be distorted, and at the same time the

$\Delta\tau i,\ \mu s$

passing instant through the zero level may be determined incorrectly. Such a situation is very difficult to be assessed.

This above mentioned problem does not occur, when the measurement is performed at the plate center. Analysis of the modeling results shown in Fig. 10-13 allows get conclusion, that zero level crossing instant determination uncertainty $U_{T0} \approx 10^{-7}$ s may be achieved. From (Eq.14) we get:

$$U_{Tx} = 2.8 \cdot 10^{-7} s \,. \qquad (15)$$

Propagation time and bending strength experimental determination

459 examples in the machine direction (MD) and 459 examples in the cross machine direction (CD) were prepared from plates manufactured at different time.

First of all the propagation time of the symmetric Lamb waves were measured, and after that the bending strength was determined using the usual destructive method. Summarized results are presented in Fig 17 and 18.

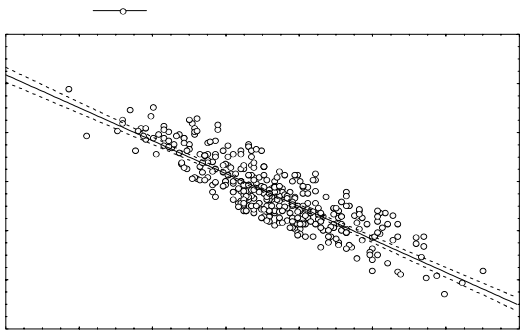

Fig. 17. **Cross correlation between the bending strength measured by the standard method and the Lamb waves propagation time measured by the hardboard strength meter in the machine-direction (n=459)**

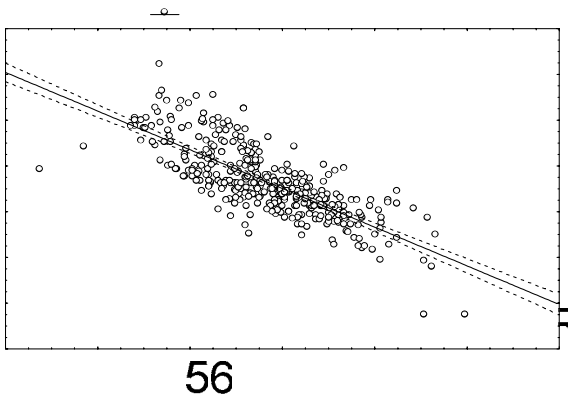

Fig. 18. **Cross correlation between the bending strength measured by the standard method and the Lamb waves propagation time measured by the hardboard strength meter in the cross-direction (n=459).**

From these experiments the following equation were obtained

$$\sigma_{MD} = 161.43 - 0.6711 \cdot T_{MD} \qquad (16)$$

and

$$\sigma_{CD} = 199 - 0.8456_{CD} \qquad (17)$$

where σ_{MD}, T_{MD} are the bending strength and the propagation time for the samples cut out in the MD; σ_{CD} , T_{CD} are the bending strength and the propagation time for the samples cut out in the CD. The obtained dependences were used in the developed measuring instrument.

Hardboard strength measuring instrument

On the basis of the obtained results the hardboard strength measurement instrument has been developed, structure of which is shown in Fig. 19.

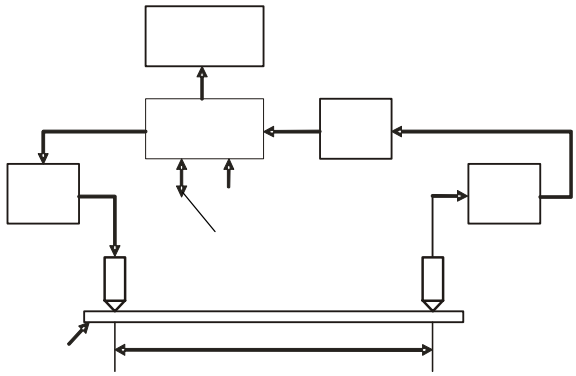

Fig. 19. **Structure of instrument for measurement of hardboard strength: G- generator; T- transmitter; R- receiver; F-former**.

Main characteristics of the measurement instrument are the following:

1. Measurement of the hardboard strength in the machine and in the cross directions.
2. Strength measurement limits 20 … 50 MPa.
3. Strength measurement uncertainty 2 MPa.
4. Ultrasonic Lamb wave propagation duration measurement limits 100 … 250 μs.
5. Memory (number of measurements) 250.

The series of measurements were carried out using the developed instrument and by standard means. Different operators at a different time carried out more than 800 measurements. For illustration the results of the first group of specimens are presented in Fig.20 and 21.

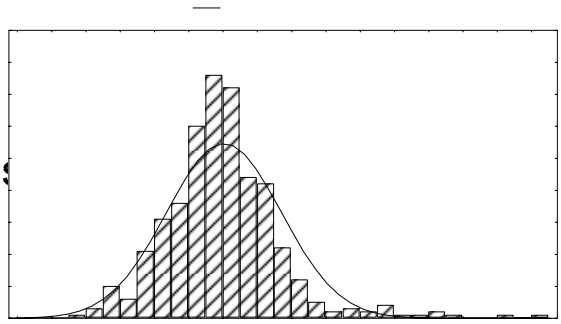

Fig. 20. **Measurements results of specimens cut out of hardboard in the machine-direction, the strength measured by the Lamb waves method (n=400)**

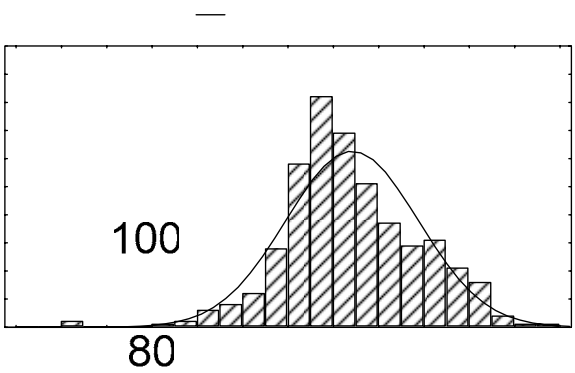

Fig. 21. **Measurements results of specimens cut out of hardboard in the machine-direction, strength measured by the standard method (n=400)**

Repeating measurements by the ultrasonic method after several months, it was noticed that the hardboard strength in the course of time increases. This result does not contradict the results obtained by the standard method.

For comparison the results obtained by the standard method and by the ultrasonic method the data are presented in Table 1.

Table 1.

Method of measurement	Strength of specimen cut of in the machine-direction of HB, MPa	Strength of specimen cut of in the cross-direction of HB, MPa
First group of specimen		
Standard method	42,82 ± 2,92	40,75 ± 3,15
Ultrasonic	42,92 ± 2,44	40,55 ± 2,29
Second group of specimen		
Standard method	42,36 ±3,56	40,16 ±4,16
Ultrasonic	42,38 ± 2,38	40,3 ± 2,84
Total measurement results		
Standard method	42,62 ± 3,23	40,55 ± 3,64
Ultrasonic	42,68 ± 2,43	40,44 ± 2,55

The difference of using total measurement results was verified by calculation the Student's criteria. If the significance level p= 0,05 (n=825) then one may affirm that the measurement results are statistically reliable for measurements in the machine-direction and in cross-direction of hardboard.

Conclusions

1. Ultrasonic strength measurement method may be used for an effective hardboard strength testing and in assessing its distribution in a panel. The method may be implemented in a line.
2. Although the main investigation was carried out on the basis of hardboard, however, the ultrasonic method may be also applied to other panels. This is proved by statistic averages of hardboard strength measurement results by the standard method breaking in two and by the ultrasonic method, which practically coincide with each other.
3. Difference of measurement results of some specimens occur due to the following causes:
   - in narrow specimens there are side reflections. Therefore, ultrasonic measurement instrument should be positioned at the centre of a specimen. When measuring in large hardboard panels, errors due to reflections were not found;
   - ultrasonic measurement method presents strength value integrated between measurement point (the distance between points was 400 mm), while the standard method presents the local strength value in the breaking place.

References

1. American society for testing and materials. D 1037-96a. Standard test methods for evaluating properties of wood-base fiber and particle panel materials. ASTM Anal Book of standards. 1996. Vol 4.10. Wood. ASTM, West Conshohocken. PA. P. 136-165.
2. **Augutis V., Dumčius A.** Hardboard strength measurement methods. ISSN 1392-1223. Measurements. Kaunas University of Technology. 2004. No 1 (29).
3. **Dumbrava V., Macas A..** Signals and systems. ISSN 9955-09-395-1. Kaunas: Technology. 2004. P. 81.
4. **Ustaski D. A., Bechtel J. K., and Gorman T. M.** Ultrasonic stress graded veneer. The international Panel and Engineering Wood Technology Exposition. Atlanta, GA. 1993.
5. **Kažys R., Stolpe P.** Ultrasonic non-destructive on-line estimation of the tensile stiffness of a running paper web. NDT and E international. 2001. Vol. 34. P. 259-267.

S. V.Augutis, A. Dumčius, D. Gailius, D. Styra, S. Jačėnas

Ultragarsinis medienos plaušo plokščių lenkiamojo stiprio bandymo metodas

Reziumė

Medienos plaušo drožlių ir skiedrų plokštės yra plačiai naudojamos įvairiose srityse. Vienu iš svarbiausių šių plokščių parametrų yra lenkiamasis stipris. Standartinis lenkiamojo stiprio matavimas atliekamas lenkiant ant dviejų atramų padėtą bandinį iki lūžimo.

Šio darbo tikslas buvo ištirti ultragarsinių Lembo bangų panaudojimo neardomajam lenkiamojo stiprio įvertinimui galimybes. Sukurti simetrinių Lembo bangų keitikliai skirti Lembo bangų greičiui arba sklidimo tarp žinomu atstumu esančių siuntiklio ir ėmiklio trukmei matuoti. Sudarytas matavimo kanalo modelis, kurį naudojant ištirta matavimo kanalo įtaka Lembo bangų sklidimo trukmės matavimo tikslumui.

Eksperimentiškai ištyrus Lembo bangų sklidimo trukmę medienos plaušo plokštėse ir jų lenkiamąjį stiprį standartiniu ardomuoju metodu, nustatyta lenkiamojo stiprio ir sklidimo trukmės priklausomybė.

Remiantis atliktais tyrimais sukurtas lenkiamojo stiprio matuoklio prototipas, įgalinantis neardomuoju būdu įvertinti plokščių lenkiamąjį stiprį ir ištirti jo pasiskirstymą išilgai ir skersai plokštės.

Pateikta spaudai 2004 12 14

DOI: 10.5755/j01.u.53.4.16909